

Rheological behavior and morphology of poly(lactic acid)/lowdensity polyethylene blends based on virgin and recycled polymers: Compatibilization with natural surfactants

Original

Rheological behavior and morphology of poly(lactic acid)/lowdensity polyethylene blends based on virgin and recycled polymers: Compatibilization with natural surfactants / Casamento, Francesco; D'Anna, Alessandra; Arrigo, Rossella; Frache, Alberto. - In: JOURNAL OF APPLIED POLYMER SCIENCE. - ISSN 0021-8995. - ELETTRONICO. - (2021), p. 50590. [10.1002/app.50590]

Availability:

This version is available at: 11583/2871532 since: 2021-02-17T15:27:08Z

Publisher:

Wiley

Published

DOI:10.1002/app.50590

Terms of use:

This article is made available under terms and conditions as specified in the corresponding bibliographic description in the repository

Publisher copyright

GENERIC -- per es. Nature : semplice rinvio dal preprint/submitted, o postprint/AAM [ex default]

The original publication is available at <https://onlinelibrary.wiley.com/doi/10.1002/app.50590> / <http://dx.doi.org/10.1002/app.50590>.

(Article begins on next page)

Rheological behaviour and morphology of PLA/LDPE blends based on virgin and recycled polymers: compatibilization with natural surfactants

Francesco Casamento, Alessandra D'Anna, Rossella Arrigo*, Alberto Frache

Department of Applied Science and Technology, Polytechnic of Turin, INSTM Local Unit, Viale Teresa Michel 5, 15121 Alessandria, Italy

*Correspondence to: Rossella Arrigo (E-mail: rossella.arrigo@polito.it)

(Additional Supporting Information may be found in the online version of this article.)

ABSTRACT

Blends based on poly(lactic acid) and low-density polyethylene were compatibilized exploiting an innovative strategy involving the introduction of different mixtures of two sustainable liquid surfactants characterized by dissimilar hydrophilic–lipophilic ratios. The compatibilization method was first applied on blends made of virgin polymers, aiming at assessing the surfactant mixture inducing a more significant morphology refinement. Besides, to verify the effectiveness of the selected compatibilizers on recycled materials, the same process was carried out on blends based on reprocessed polymers. Interestingly, the compatibilization caused a significant microstructure modification, with a decrease of 54% of the mean size of the dispersed particles, in the case of virgin polymers-based blends, with a consequent increase of 19% of the dynamic elastic modulus. On the other hand, in the case of reprocessed polymers-based blends, a different compatibilizer efficiency was observed, as the non-compatibilized blend showed a more regular microstructure compared to the compatibilized counterpart.

INTRODUCTION

In recent years, the impact of plastic pollution has been increasingly noticeable, due to the accumulation of plastic waste in the seas, which is causing serious harm to the sea wildlife. Therefore, with the aim to reduce the quantity of plastic waste, both scientific research and government authorities are looking for more sustainable alternatives compared to the traditional thermoplastics [1].

A method that has been exploited for several years is the recycle of plastic waste [2]. Recycling involves different strategies: chemical, energetic, and mechanical [3]; in this latter case, waste coming either from production scraps (primary recycling) or from end-of-life products (secondary recycling) is grounded and used as secondary raw material. Most of the traditional thermoplastics, such as polyethylene terephthalate (PET) [4], polypropylene (PP) [5], high-density polyethylene (HDPE) [6] and low-density polyethylene (LDPE) [7] undergo mechanical recycling. Although this strategy represents an economic and feasible way to recover plastic waste, it presents some limitations. First, the main issue of mechanical recycling is the loss of properties that plastic waste experienced during the reprocessing cycles, since the energy or heat supply can induce degradation of the polymers, with a detrimental effect on the material final properties. Furthermore, the quality of the final material is strictly related to the processes of separation, washing and preparation of plastic waste prior to mechanical treatment [3].

A second alternative to the consumption of traditional plastic materials is the use of biodegradable polymers; in this way, it is possible to use materials with similar properties to those of traditional thermoplastics but with the advantage of an easier disposal. Biodegradable polymers derived from both renewable [8-10] and combustible sources [11-12], are nowadays

used in different applications. In particular, poly(lactic acid) (PLA) is one of the most exploited biopolymers as an alternative to traditional thermoplastics, due to its mechanical properties comparable to those of traditional thermoplastics, its biodegradability and biocompatibility, as well as for the huge availability of renewable sources from which it is produced. The main limitation of PLA, however, is its high fragility, which makes it unsuitable for many industrial applications [13]. For this reason, it is often necessary to create polymer blends between PLA and a more ductile polymer [14]. In general, the formation of a polymeric blend aims at developing a material with required properties, which are difficult to obtain from single polymers [15]. However, due to thermodynamic issues, most polymers are not miscible, and the final blends exhibit a biphasic morphology, compromising the properties of the final material [16]. To overcome this disadvantage, a compatibilization action is therefore required; most common compatibilization methods involve the insertion of a compatibilizing agent, able to induce a decrease of the interfacial tension between the two polymeric phases, with the consequent achievement of a more refined and stabilized morphology [17]. In order to improve the compatibility between PLA and other polymers, several strategies of compatibilization have been employed, as reported in different studies [18]. Amongst the different developed techniques, one of the most used is the addition of block copolymers, featuring one block compatible with PLA and the other to the second component. In this context, Wang et al. employed PLA-PE diblock copolymers in the compatibilization of PLA/PE blends [19]. Another commonly used technique of compatibilization is the addition of nanoparticles, which locate at the interface between the two components, improving the interfacial adhesion and therefore the properties of the blend. An

example is provided by the work of Chen et al., who evaluated the effect of twice functionalized organoclay (TFC) on the compatibility in the blend PLA/PBS. [20].

Various examples of blends between PLA and other polymers are reported in literature, either based on biodegradable polymers, such as poly(hydroxy butyrate) [21] and starch [22], or non-biodegradable materials, like polypropylene [23] and polyethylene [24-26]. In particular, blends between PLA and LDPE were developed, aiming at increasing the toughness of PLA. Researches about PLA/LDPE blends showed the immiscibility between the two polymers, so that compatibilization was required to obtain a final material endowed with superior properties. In this context, Kim et al. [24] and Anderson et al. [25] examined the compatibilization of PLA/LDPE blends using copolymers as compatibilizing agents.

In this work, PLA/LDPE blends were produced through melt-mixing, and the morphology, rheology and thermomechanical behavior of the resulting materials were evaluated. Besides, a compatibilization method involving the introduction of a mixture of two natural surfactants was applied. The development of blends based on biodegradable and fossil fuel-based polymers can gain particular interest considering that the rising utilization of biodegradable polymers as an alternative to traditional fossil fuel-based thermoplastics in several application fields, involves the presence of increasing amounts of these polymers into the waste stream mainly composed of polyolefins, affecting the final properties of the material subjected to mechanical recycling operations. The developed materials were obtained using both virgin and reprocessed polymers as feedstock, aiming verifying the effectiveness of the selected compatibilization strategy also on materials underwent mechanical recycle operations, which could be potentially suitable for different commercial applications, such as the formulation of packaging materials or houseware.

EXPERIMENTAL

Materials

Poly(lactic acid) (PLA) (trade name: Ingeo™ 3251D) was supplied in pellets by Ingeo™ Natural Natureworks (Minnetonka, MN, USA). Polymer main properties are: density = 1.24 g/cm³, MFI = 33 g/10 min (190 °C, 2.16 kg). Low-density polyethylene (LDPE) was supplied in pellets by Repsol (Madrid, Spain) under trade name ALCUDIA® PE022; its main properties are: density = 0.915 g/cm³, MFI = 70 g/10 min (190 °C, 2.16 kg). Tween TM 80-LQ-(CQ) is an ethoxylated sorbitan ester, while Span TM 80-LQ-(RB) is a sorbitan ester; both additives were supplied by CRODA and are bio-based non-ionic surfactants in liquid state. Acetone was supplied by SIGMA-ALDRICH, laboratory reagent >99.5%, and it was used as received.

Preparation of PLA/LDPE blends

PLA pellets were first dried overnight at 70 °C in a vacuum oven. Blends were then prepared using a DSM Explore twin screw mini-extruder. Adopted process parameters were: T = 190 °C, screw speed = 50 rpm (during addition of pellets), 100 rpm (during mixing), 70 rpm (extrusion), mixing time = 2 minutes at 100 rpm, protective Nitrogen atmosphere. Non-compatible PLA/LDPE blends at different weight ratios were prepared; obtained blends were designed as PLA/LDPE X/Y, where X and Y indicate PLA and LDPE content (wt.%), respectively.

Since the studied blends were composed by polymers having polar and non-polar character, it was considered appropriate to use as compatibilizer a mixture of the two additives with different compositions. To this aim, two sustainable surfactants, namely Tween 80 and Span 80 with hydrophilic and hydrophobic character, respectively, were mixed at different weight ratios to

obtain a mixture characterized by a certain HLB (Hydrophile-Lipophile Balance), accounting for the balance of the size and strength of the hydrophilic (polar) and the lipophilic (non-polar) groups of the surfactant. When two or more emulsifiers are blended, the resulting HLB of the blend is calculated using the mixing rule [26]. HLB indices of pure Tween 80 and Span 80 are 15 and 4.3, respectively; the selected mixtures with different weight ratios of surfactants and thus different HLB indices are reported in Table 1. In particular, the HLB 12 index was chosen in order to have mixtures of surfactants presenting a ratio between hydrophilic and hydrophobic character similar to the weight ratio between the polymer having polar behavior – PLA – and the polymer with non-polar behavior – LDPE. The other two mixtures having HLB 10 and 9 were formulated in order to have a neutral balance between the hydrophilic and lipophilic content.

TABLE 1 HLB and composition of the used surfactant mixtures.

Surfactants mixture HLB	Tween 80 (wt%)	Span 80 (wt%)
12	72	28
10	54	46
9	44	56

The blend which was selected to be compatibilized was PLA/LDPE 70/30; the two surfactants were first manually mixed and then dissolved in about 5 ml acetone, to be added more easily in the mini extruder chamber. The surfactant mixtures were added at 1% wt.

Furthermore, the blends PLA/LDPE 70/30, both uncompatibilized and compatibilized with the mixture having HLB 12, were prepared using recycled polymers; the term “recycled” indicates that polymers underwent two extrusion cycles. These blends made of recycled polymers are listed in the following:

1. Blend r-PLA/r-LDPE 70/30. Polymers were first extruded alone and finally blended together in the second extrusion.
2. Blend r-PLA/r-LDPE 70/30 HLB 12. Polymers were first extruded alone and then mixed together with the addition of the compatibilizer at 1% wt in the second extrusion.

The specimens used for thermomechanical and rheological characterizations were obtained by compression molding, using a Collin P 200 T press (operating at 210 °C under a pressure of 100 bar).

Characterizations

Differential scanning calorimetry (DSC) measurements were carried out on samples of about 8 mg, placed in sealed aluminum pans, using a Q20 TA Instrument (TA Instruments Inc., New Castle, DE, USA). All the experiments were performed under dry N₂ gas (20 mL/min). The samples underwent the following cycle: a heating ramp from –50 to 200 °C to eliminate the thermal history of the sample, a cooling ramp from 200 to –50 °C, and then a second heating step from –50 to 200 °C. All the heating/cooling ramps were performed at a scanning rate of 10 °C/min.

Thermomechanical measurements (DMA) tests were performed using a Q800 TA Instrument (TA Instruments Inc., New Castle, DE, USA) equipped with tension film clamps. Samples with dimensions of 6 mm width × 26 mm height × 1 mm thickness were used. The temperature was varied in the range from 30 to 95 °C, applying a heating rate of 3 °C/min. The test conditions were: 1 Hz of frequency in strain-controlled mode with 15 mm of amplitude, static loading of 125% of dynamic loading, and 0.01 N of preload. Samples were dried in a vacuum oven for 70 °C overnight before carrying the tests. Thermomechanical tests were carried out on 3 different samples.

Rheological tests were performed on rheometer ARES TA Instrument (TA Instruments Inc., New Castle, DE, USA) in parallel plate geometry, with a plate diameter of 25 mm, under nitrogen atmosphere to avoid polymer oxidative degradation. Complex viscosity (η^*) and elastic (G') and loss (G'') moduli were measured performing frequency scans from 0.1 to 100 rad/s at 190 °C. The strain amplitude was selected for each sample in order to fall in the linear viscoelastic region. The typical gap between the plates imposed during the tests was 1 mm. Prior to the measurements, the samples were vacuum-dried at 70 °C overnight.

The morphology of the blends was observed using a LEO-1450VP Scanning Electron Microscope SEM (beam voltage: 20 kV). The observations were performed on the fracture surfaces of the samples, obtained through fracturing in liquid nitrogen. Before the tests, the fracture surfaces were coated with a thin gold layer.

RESULTS AND DISCUSSION

Non-compatibilized PLA/LDPE blends

A preliminary analysis on PLA/LDPE non-compatibilized blends was first performed; to this aim, several PLA/LDPE blends with different compositions were developed. The analysis of the thermal behavior of the formulated blends was carried out to verify the immiscibility of studied systems (recorded thermograms are reported in Supplementary Information, Figure S1). In all produced blends, the peaks corresponding to glass transition and cold crystallization temperature of PLA and to the melting points of both LDPE and PLA, are almost unchanged with respect to those of pure polymers. It is known from literature [15] that the invariance of the glass transition temperature is a proof of the immiscibility between the two polymers; therefore, it is possible to infer the immiscibility between PLA and LDPE for each selected composition.

As none of the studied compositions showed significant variations of characteristic temperatures compared to the pure polymers, it was decided to concentrate the study on the blend PLA/LDPE 70/30, in order to draw the attention of the study on a system having PLA as the primary phase, as it was discussed in our previous work [21].

Since rheology is a powerful tool to investigate the morphology of polymeric blends, small amplitude oscillatory shear measurements were carried out on the blend PLA/LDPE 70/30 and on the pure polymers. Figure 1A shows the variation of the viscosity as a function of frequency for the pure polymers and for the blend PLA/LDPE 70/30. PLA exhibits a well-pronounced Newtonian rheological behavior, with viscosity showing a plateau at low-intermediate frequency values; conversely, the rheological behavior of LDPE is remarkably non-Newtonian, as the shear-thinning region extends over all the investigated frequency range. The evolution of the viscosity curve of the blend is different from what observed for pure polymers; in particular, the blend shows viscosity values intermediate between those of pure polymers at high frequencies, but higher values in the low frequency range. Figure 1B reports the evolution of the storage modulus as a function of frequency for pure polymers and the blend. Neat polymers exhibit the typical behavior of homopolymers; in the blend the values of G' are intermediate between those of the polymers at high frequencies but become much higher at low and intermediate frequencies. The different rheological response of the blend compared to the pure polymers is attributable to the biphasic morphology of the material; in particular, the creation of interfaces between the two polymers and the occurrence of phenomena of shape relaxation of the dispersed particles during oscillatory shear flow, result in an excess elasticity, which induces the increase of both viscosity and storage modulus as compared to the pure polymers. This feature is more pronounced in the

low frequency region, where the response of large portions of macromolecules is recorded; conversely, at higher frequencies, the effect is less remarkable, since the curves reflect the response of small fraction of polymer chains, associated with a dynamic population that relax faster, and the rheological behavior is governed by pure polymers [27].

The morphology of the blend PLA/LDPE (70/30) was evaluated through SEM observations. Representative micrographs, reported in Figure 1(C-D), clearly show that the material exhibits the typical morphology of an immiscible polymeric blends [16], with particles of the minor phase (LDPE) dispersed in a continuous matrix of the major phase (PLA). The dispersed droplets, whose size distribution is reported in Figure 1E, show a wide range of dimensions; in particular, the fitting of experimental data with a Gauss-like distribution curve, highlighted the appearance of three main peaks, centered at about 45, 65 and 85 μm , indicating the heterogeneity of the blend morphology; the mean size of the particles is 88.14 μm . Furthermore, from SEM observations it can be noticed that the interfaces between the two phases are very clear, and many holes along the fracture surface can be detected, suggesting a weak interfacial adhesion between the two polymers.

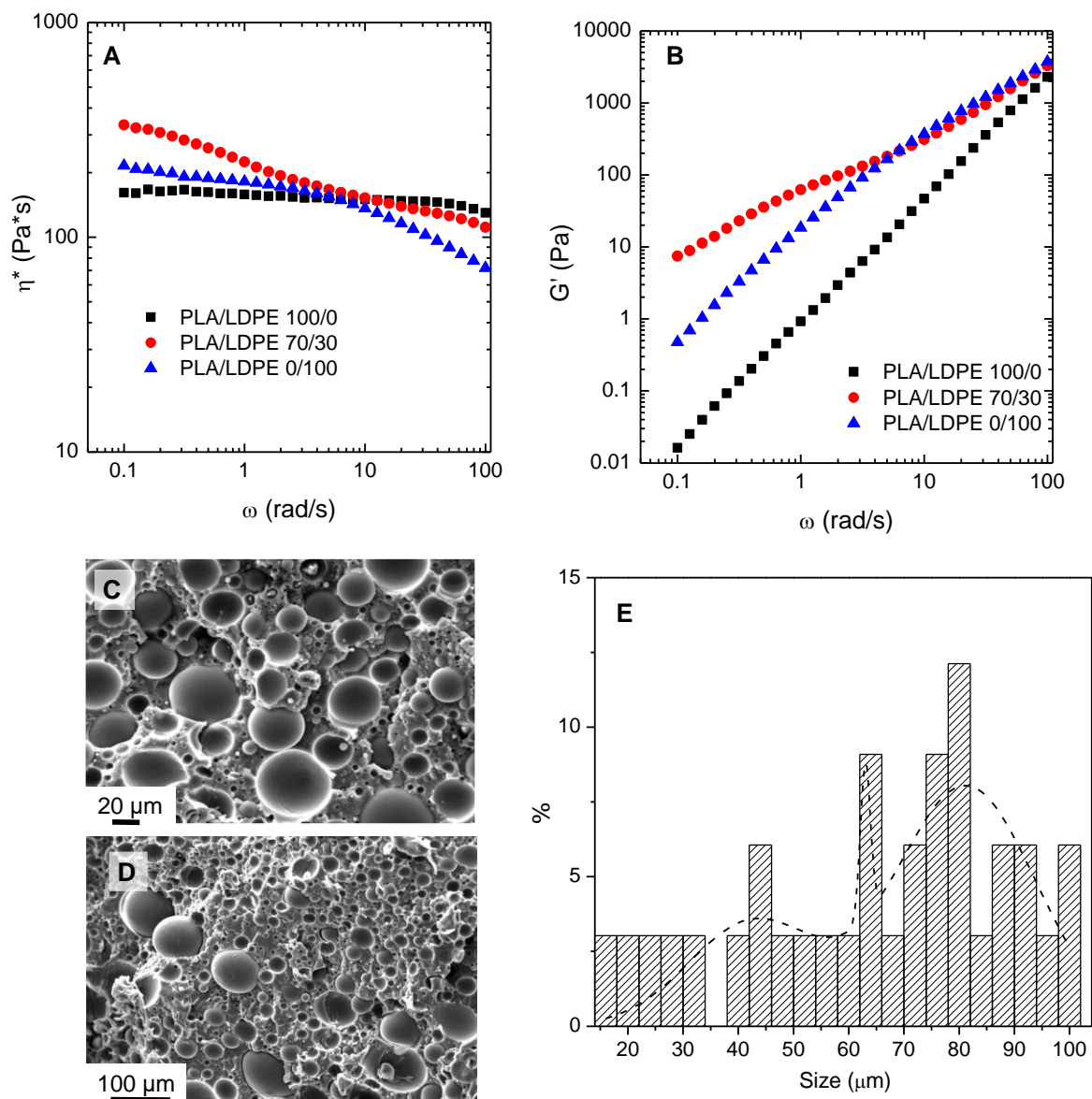


Figure 1 (A) Complex viscosity and (B) storage modulus curves as a function of frequency for PLA/LDPE 70/30 blend and pure polymers; (C-D) SEM micrographs of PLA/LDPE 70/30 blend at different magnifications and (E) related size distribution of the dispersed particles.

Compatibilized PLA/LDPE 70/30 blends

The main goal of the compatibilization of the blend was to improve the miscibility between the two polymers, in order to achieve a material with enhanced final properties. In fact, the introduction of a compatibilizing agent causes the reduction of the interfacial tension and promotes the interfacial adhesion between the two phases, resulting in a finer dispersion of the dispersed particles and a stabilization of the morphology, as well.

The thermal analysis performed on PLA/LDPE 70/30 compatibilized blends (thermograms are reported in Figure S2) highlight a reduction of about 2 °C of the values of T_g for the systems containing the different compatibilizers (HLB = 9, 10, 12), as compared to the uncompatibilized blend, suggesting an improvement of the miscibility between the two polymers [28].

Figure 2A reports the variation of storage modulus G' as a function of frequency for all compatibilized blends, compared to that of uncompatibilized PLA/LDPE 70/30 system. All investigated blends, both uncompatibilized and compatibilized, exhibit similar rheological response, and the shoulder-like behavior of the storage modulus suggests that the morphology of compatibilized blends remains droplet-like, also in presence of compatibilizers.

Dynamic thermomechanical analyses were carried out to verify the effect of the compatibilizer mixture on the mechanical properties of the blend. Figure 2B reports the variation of the dynamic storage modulus E' as a function of the temperature, for uncompatibilized and compatibilized PLA/LDPE 70/30 blends. Amongst the used surfactants, the mixture having HLB 12 induces the most significant improvement of the elastic modulus; in fact, at 35 °C, the dynamic storage modulus of the blend 70/30 HLB 12 reaches the value of 1870 MPa, bringing to an increase of 19% with respect to the non-compatibilized blend, which exhibits values of E' of 1570 MPa. The

improvement of the storage modulus was less pronounced in the case of the blends with other compatibilizers mixtures; in fact, these materials present values E' of about 1650 MPa, showing an increase of 5% compared to the non-compatibilized blend.

In Figure 2C, the variation of $\tan \delta$, representing the ratio between the dynamic loss modulus, E'' , and E' , as a function of the temperature is reported. The peak of the damping curves occurs for the compatibilized blends at slightly lower temperatures (84 °C) as compared to uncompatibilized material (85 °C); furthermore, broader peaks are obtained for compatibilized systems, indicating the achievement of a partial miscibility between the polymeric components [29] and an improved dispersion of the LDPE phase, inducing the achievement of a larger interfacial surface between the two phases [30].

According to these results, it is possible to suppose that the blend 70/30 HLB 12 should exhibit a more refined morphology, with smaller dispersed particles and less evident interfaces between the two phases. The morphology of the blend PLA/LDPE 70/30 HLB 12, which was the one with the highest improvement of storage modulus, was investigated through SEM analysis, which confirms the results of DMA analyses, as a significant reduction of the average dimension of the particles of the dispersed phase was observed. In fact, the measured mean size of the dispersed particles is 40.19 μm , meaning a reduction of 54% compared to the dimensions of the dispersed particles in the non-compatibilized blend. In Figure 2D, the size distribution of the droplets constituting the dispersed phase for the PLA/LDPE 70/30 HLB 12 system is reported (red curve), along with the distribution curve of the uncompatibilized blend (dashed line). A significant beneficial effect of the HLB 12 presence on the morphology homogeneity can be clearly observed since, in the case of compatibilized system, the distribution curve exhibits two sharp peaks

centered at about 12 and 38 μm , with a remarkable decrease of the maximum droplet size as compared to the uncompatibilized blend.

Figure 3 shows the supposed mechanism of compatibilization, involving the preferential localization of the surfactant molecules in the interfacial region between the two polymeric phases. More specifically, the hydrophilic group of the surfactant mixture interacting with the polar PLA matrix, and the lipophilic parts directed towards the non-polar dispersed droplets of LDPE, are able to induce a refinement of the blend morphology, notwithstanding the presence of many holes in the surface of fracture, as well as pronounced interfaces between continuous and dispersed phases, indicating that the adhesion between the two phases remained weak.

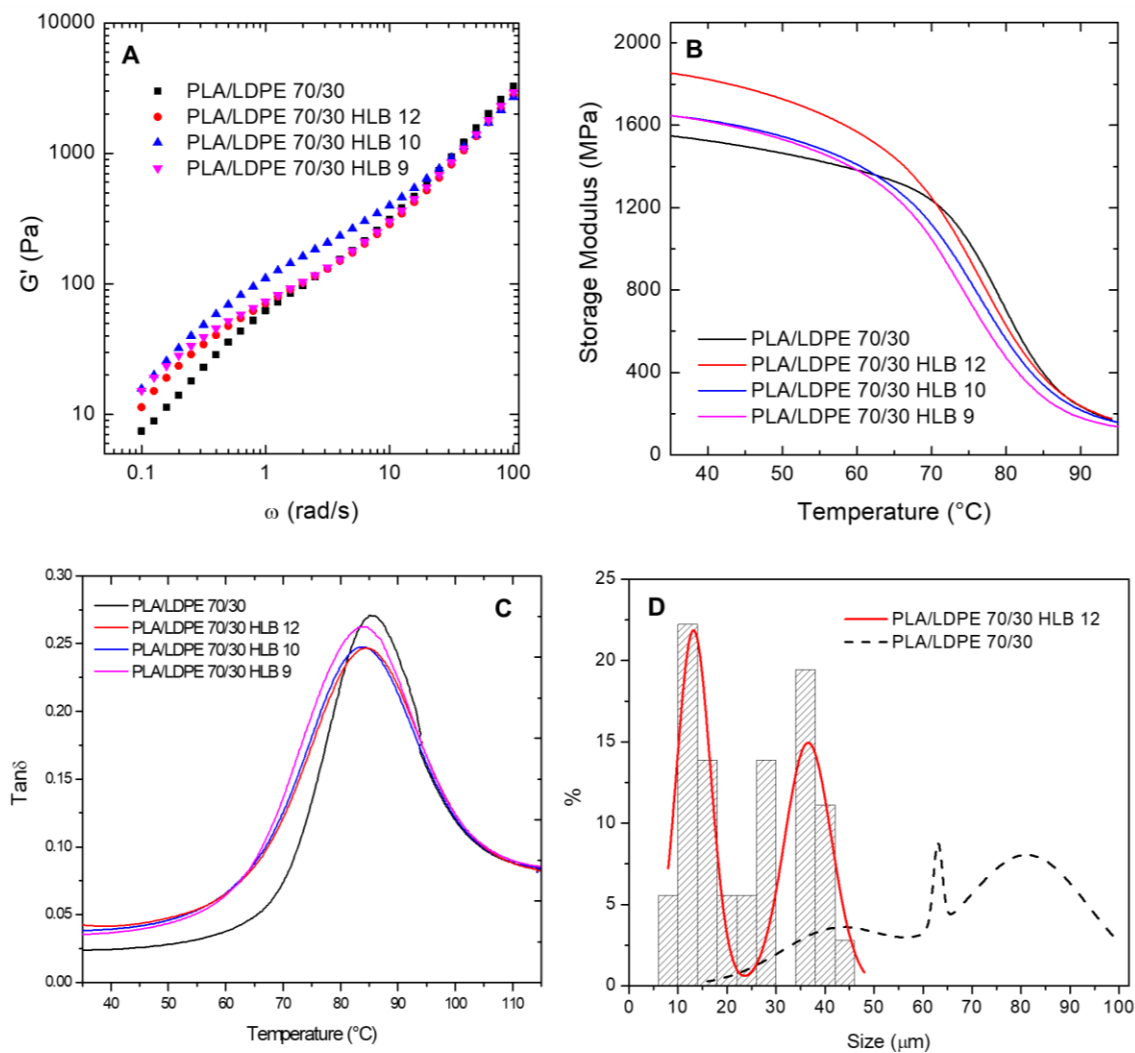


Figure 2 (A) Storage modulus as a function of frequency, (B) dynamic storage modulus and (C) $\tan\delta$ traces of uncompatibilized and compatibilized PLA/LDPE 70/30 blends; (D) size distribution of the dispersed particles of PLA/LDPE 70/30 HLB 12 system

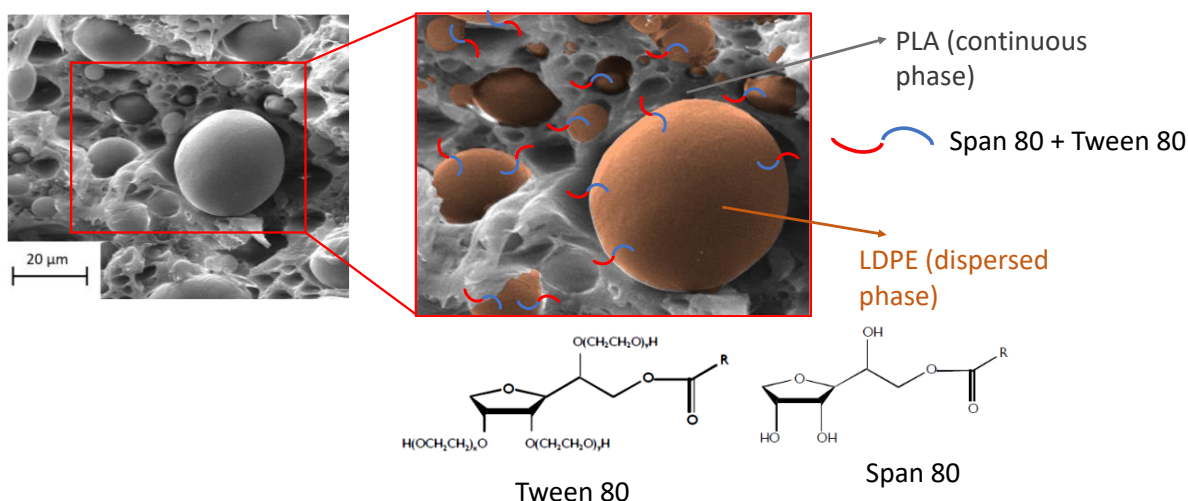


Figure 3 Compatibilization mechanism of the blends and SEM micrograph of the blend

PLA/LDPE 70/30 HLB 12

Recycled blends

The main aim of this study was to verify the effectiveness of the compatibilization strategy exploited for the blend PLA/LDPE 70/30, based on virgin polymers, also on blend of the same composition but composed of recycled polymers, named r-PLA/r-LDPE 70/30. The compatibilizer mixture which was used in this second part of the study was the one having HLB 12, as this mixture brought to the higher improvements over the uncompatibilized blend, in the case of materials based on virgin polymers.

Similarly to what observed for virgin polymers-based blends, the introduction of the compatibilizer mixture causes the decrease of the value of the glass transition temperature (DSC thermograms and Tg values are reported in Figure S3 and Table S3, respectively).

Figure 4A reports the trend of the dynamic storage modulus E' as a function of temperature for recycled polymers-based blends, along with the curve of uncompatibilized PLA/LDPE system. The

uncompatibilized blend developed from recycled polymers presents higher values of E' as compared to the blend based on virgin polymers, and this finding can be related to the improved compatibility between the polymers, whose molecular weights could have been decreased due to the reprocessing [31]. In fact, as reported in literature [32], the decrease of molecular weight would bring to a reduction of interfacial tension between the two phases. As far as r-PLA/r-LDPE 70/30 HLB 12 is concerned, differently from the case of blends based on virgin polymers, the adopted compatibilization method was not effective in inducing an improvement of the mechanical properties with respect to the uncompatibilized blend, as the r-PLA/r-LDPE 70/30 HLB 12 material showed lower storage modulus at low temperatures. These results seem to suggest that a better morphology has been obtained in the non-compatibilized blend.

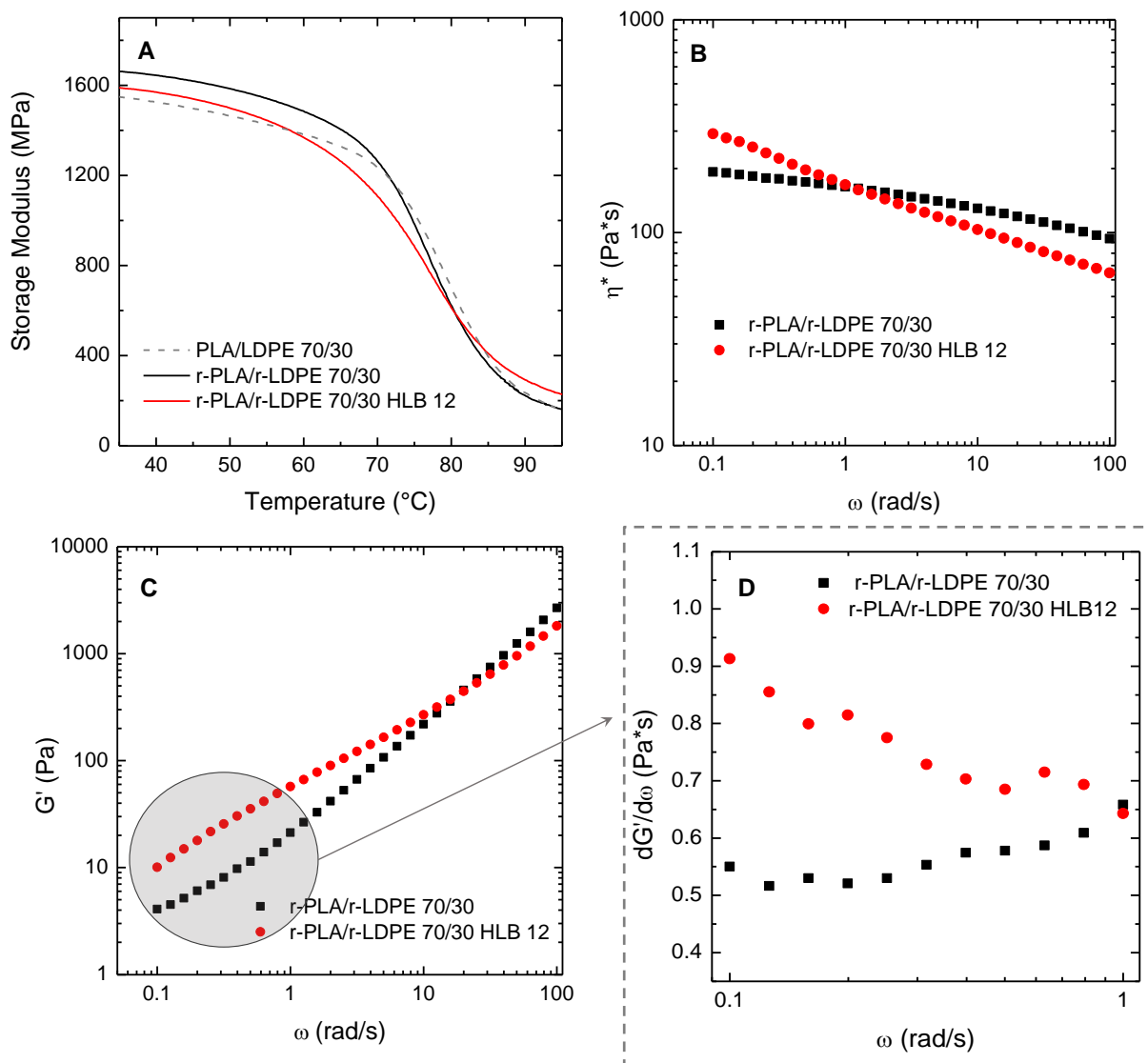


Figure 4 (A) DMA traces, (B) complex viscosity, (C) storage modulus, (D) $dG'/d\omega$ curves as a function of frequency for recycled polymers-based blends.

To verify this finding, frequency sweep measurements have been carried out and obtained results are reported in Figures 4B-D. Firstly, both recycled blends showed lower values of viscosity as compared to the blends based on virgin polymers, indicating that the reprocessing caused a

decrease of polymer molecular weight and, consequently, of the viscosity. Furthermore, the two blends exhibit very different viscoelastic behaviors, in terms of both viscosity and storage modulus. As far as the viscosity trend is concerned, from results reported in Figure 3B it is evident that the compatibilized blend exhibits a well-pronounced non-Newtonian behavior. The difference between the viscoelastic behavior of the two materials is even more evident looking at the curves of G' , shown in Figure 4C. More specifically, the compatibilized blend shows, similarly to what observed in the case of blends based on virgin polymers, the typical trend of an immiscible blend, with the presence of a shoulder at low and intermediate frequencies, associable with the relaxation phenomena of dispersed particles. Differently, for the blend r-PLA/r-LDPE 70/30 the shoulder in the storage modulus trend is not present, and a significant reduction of the slope of G' in the low frequency region can be observed. As documented in literature [21], this finding can be ascribed to the formation of complex morphologies showing slow relaxation dynamics. To deeply investigate this behavior, the slope of the G' curve ($dG'/d\omega$) at low frequencies was calculated, and its variation as a function of frequency is reported in Figure 4D. r-PLA/r-LDPE 70/30 HLB 12 blend shows a continuous decrease of the G' slope as a function of the frequency, indicating the relaxation of a single dynamic population related to the droplets constituting the dispersed phase. Conversely, the curve of the uncompatibilized blend remains almost constant as the frequency increases, reflecting the relaxation of LDPE particles of different shapes and dimensions that, relaxing continuously over a long time interval, generate a continuous spectrum of relaxation times.

Finally, the morphology of the two blends was investigated using SEM analysis and representative micrographs are reported in Figures 5A-B. r-PLA/r-LDPE 70/30 material presents a biphasic

morphology, but the dimensional distribution of the dispersed particles is relatively narrow; furthermore, the fracture surface did not exhibit a large number of holes, suggesting higher interfacial adhesion compared to the blends obtained with virgin polymers; this is consistent with the hypothesis of a decrease of molecular weight, which would bring to a reduction of interfacial tension between the two phases [32]. The addition of the compatibilizer causes the formation of many small particles, showing lower size compared to the non-compatibilized blend, but the presence of coarse-elongated particles of much higher size can be noticed; the appearance of these irregular structures could be due to coalescence phenomena of dispersed particles occurring during the processing in the presence of the compatibilizer. The morphological observations suggest that the compatibilization effectively induces the reduction of the dimension of the dispersed particles, similarly to the blends obtained from virgin polymers, but this morphological refinement is not uniform in the material. This phenomenon could be attributed to the adopted processing conditions, such as mixing time or concentration of compatibilizer, which could be not optimal in the case of the blends based on recycled polymers.

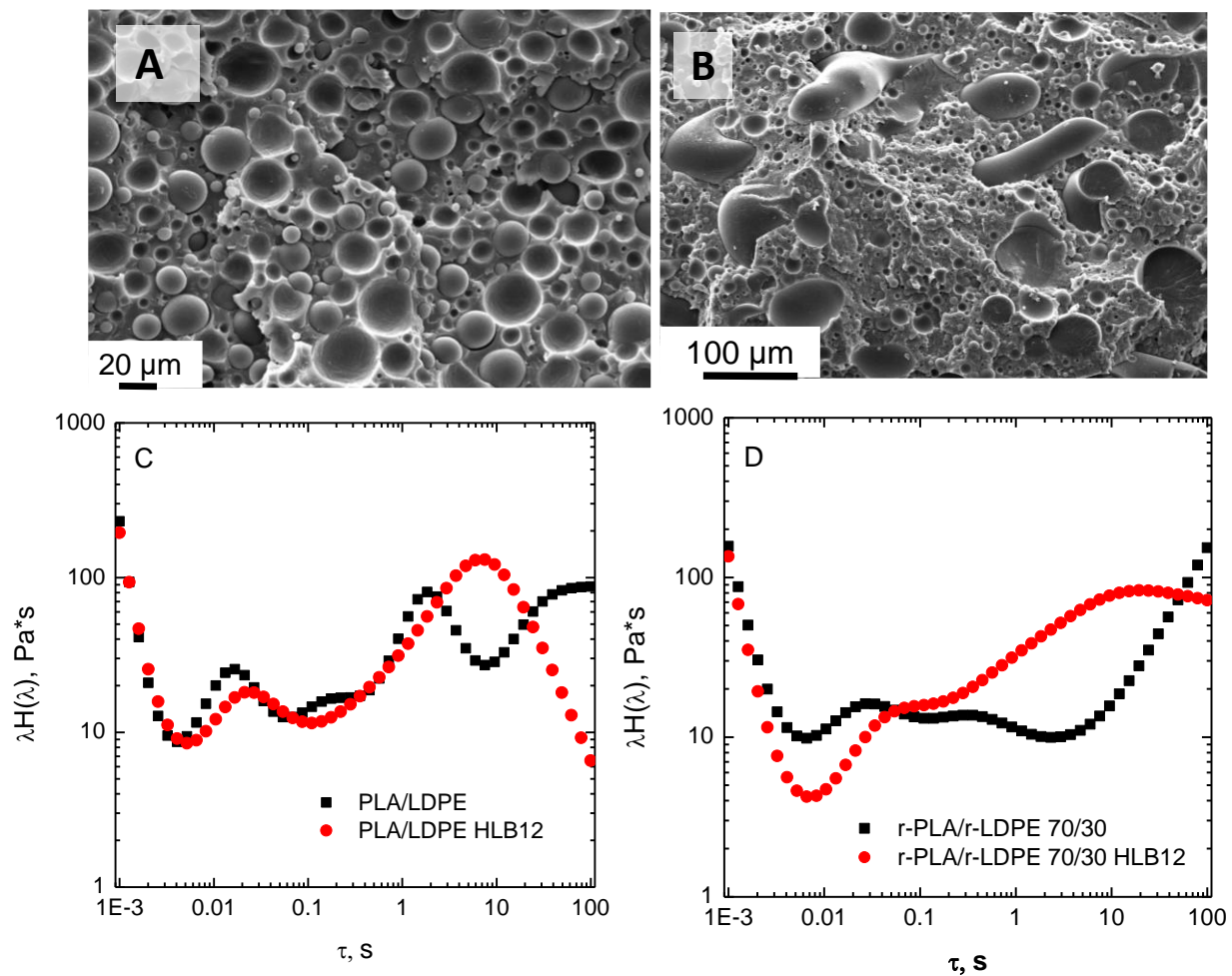


Figure 5 SEM micrographs for (A) uncompatibilized and (B) compatibilized r-PLA/r-LDPE 70/30 blends; weighted relaxation spectra for blends based on (C) virgin and (D) recycled polymers.

Results coming from morphological observations were confirmed by the analysis of the weighted relaxation spectra of uncompatibilized and compatibilized blends, which allows measuring the relaxation times associated with microstructural changes in multi-component polymer-based systems. The weighted relaxation spectrum ($\lambda H(\lambda)$) can be calculated using data coming from

small amplitude oscillatory shear measurements, using the method proposed by Honerkamp and Weese [33]. Generally, for a polymer blend, peaks appearing at short relaxation times were attributed to the relaxation processes of the blend constituents, while on the right side of the spectrum, signals observed at longer times are related with the relaxation of the blend interface [34]. Looking at the spectra reported in Figure 5C, PLA/LDPE blend exhibit three different peaks: the first one related to the relaxation of blend components, the second one attributable to the shape-relaxation of the LDPE dispersed droplets, and a peak not completely formed at longer times, associable with the presence of a population of droplets having larger size, which were not able to fully relax in the tested time interval. In the compatibilized material, the presence of HLB 12 caused the disappearance of the peak at long relaxation times, indicating a beneficial effect of the compatibilizer in obtaining a more homogeneous morphology.

Spectra reported in Figure 5D depict a different scenario for r-PLA and r-LDPE based blends. More specifically, in the uncompatibilized r-PLA/r-LDPE system the intensity of the peak related to the blend constituent is remarkably reduced as compared to the PLA/LDPE blend, indicating a viscous dominant behavior involving faster relaxation modes of the polymer chains [35]. Besides, the tail appearing at longer relaxation times can be attributed to the relaxation of the droplets constituting the dispersed phase, characterized by a continuous distribution of shapes and interface curvatures [36]. Conversely, the relaxation behavior of the r-PLA/r-LDPE HLB 12 blend involves the appearance of a broad peak at long relaxation times, associable with the presence of the elongated structures observed through SEM observations, resulting from some coarsening phenomenon, which are not able to fully relax in the investigated time interval.

CONCLUSIONS

In this study, a compatibilization method based on the use of natural surfactants was evaluated for PLA/LDPE blends, formulated using both virgin and recycled polymers. The blends were melt-mixed using a mini-extruder and then characterized through DSC, DMA, rheological analyses, and SEM. A preliminary analysis carried out on the blends made of virgin polymers showed the complete immiscibility between the two polymers at every selected composition, as demonstrated by the rheological behavior, DSC results and the morphology of the material. The addition of the compatibilizer caused a slight reduction of PLA characteristic temperatures of about 2 °C, both in virgin polymers- and in recycled polymers-based blends. In particular, the addition of surfactants mixture having HLB 12 brought to the most significant improvements of storage modulus in the blends made of virgin polymers, causing an improvement of 19% of the values of the modulus, as well as a remarkable decrease of the size of the particles of the dispersed phase, as the observed reduction of the size amounted to 54% compared to the non-compatibilized blend. Conversely, the same operating conditions of compatibilization did not induce to the same improvements in the case of the blend having same composition but made of recycled polymers, as the compatibilized blend showed lower values of E' and a more irregular morphology, presenting both small and coarse-elongated particles of dispersed phase, compared to the non-compatibilized blend. Furthermore, the blend with composition PLA/LDPE 70/30 exhibited higher values of E' , better rheological behavior and a more refined morphology when developed with recycled polymers rather than with virgin polymers, suggesting an improved compatibility between re-processed polymers.

REFERENCES

1. Adhikari, B.; De, D.; Maiti, S. *Progr. Polym. Sci.* **2000**, *25*, 909–948.
2. Scott, G. *Polym. Degrad. Stab.* **2000**, *68*, 1–7.
3. Al-Salem, S.M.; Lettieri, P.; Baeyens, J. *Waste Manag.* **2009**, *29*, 2625–2643.
4. Welle, F. *Resour. Conserv. Recy.* **2011**, *55*, 865–875.
5. Corvaglia, P.; Passaro, A.; Manni, O.; Barone, L.; Maffezzoli, A. *J. Thermoplast. Compos. Mater.* **2006**, *19*, 731–745.
6. Adhikary, K. B.; Pang, S.; Staiger, M. P. *Compos. Part. B Eng.* **2008**, *39*, 807–815.
7. Hamad, K.; Kaseem, M.; Deri, F. *Polym. Degrad. Stab.* **2013**, *98*, 2801–2812.
8. Castro-Aguirre, E.; Iñiguez-Franco, F.; Samsudin, H.; Fang, X.; Auras, R. *Adv. Drug Deliv. Rev.* **2016**, *107*, 333–366.
9. Sudesh, K.; Abe, H.; Doi, Y. *Progr. Polym. Sci.* **2000**, *25*, 1503–1555.
10. Mohammadi Nafchi, A.; Moradpour, M.; Saeidi, M.; Alias, A.K. *Starch/Stärke* **2013**, *65*, 61–72.
11. Na, Y. H.; He, Y.; Shuai, X.; Kikkawa, Y.; Doi, Y.; Inoue, Y. *Biomacromolecules* **2002**, *3*, 1179–1186.
12. Fujimaki, T. *Polym. Degrad. Stab.* **1998**, *59*, 209–214.
13. Yokohara, T.; Yamaguchi, M. *Europ. Polym. J.* **2008**, *44*, 677–685.
14. Jiang, L.; Wolcott, M.P.; Zhang, J. *Biomacromolecules* **2006**, *7*, 199–207.
15. Utracki, L.A.; Wilkie, C. A. *Polymer Blends Handbook Second Edition*. Dordrecht: Springer Science + Business Media, **2014**.
16. Xue, L.; Zhang, J.; Han, Y. *Progr. Polym. Sci.* **2012**, *37*, 564–594.
17. Petruš, J.; Kučera, F.; Jančář, J. *J. Appl. Polym. Sci.* **2019**, 48005.
18. Zeng, J.B.; Li, K.A.; Du, A.K. *RSC Advances* **2015**, *5*, 32546–32565.
19. Wang, Y.B.; Hillmyer, M.A. *J. Polym. Sci. Part A: Polym. Chem.* **2001**, *39*, 2755–2766.
20. Chen, G.X.; Kim, H.S.; Kim, E.S.; Yoon, J.S. *Polymer* **2005**, *46*, 11829–11836.
21. D’Anna, A.; Arrigo, R.; Frache, A. *Polymers* **2019**, *11*, 1416.
22. Huneault, M.A.; Li, H. *Polymer* **2007**, *48*, 270–280.
23. Aghjeh, M. R.; Kazerouni, Y.; Otadi, M.; Khonakdar, H. A.; Jafari, S. H.; Ebadi-Dehaghani, H.; Mousavi, S. H. *Compos. Part B Eng.* **2018**, *137*, 235–246.
24. Kim, Y. F.; Choi, C. N.; Kim, Y. D.; Lee, K. Y.; Lee, M. S. *Fibers Polym.* **2004**, *5*, 270–274.
25. Anderson, K. S.; Lim, S. H.; Hillmyer, M. A. *J. Appl. Polym. Sci.* **2003**, *89*, 3757–3768.
26. ICI Americas, Inc. *The HLB system: a time-saving guide to emulsifier selection*. Wilmington, **1984**.
27. Arrigo, R.; Bartoli, M.; Malucelli, G. *Polymers* **2020**, *12*, 892.
28. Abdelwahab, M. A.; Flynn, A.; Chiou, B.S.; Imam, S.; Orts, W.; Chiellini, E. *Polym. Degrad. Stab.* **2012**, *97*, 1822–1828.
29. Komalan, C.; George, K. E.; Kumar, P. A. S.; Varughese, K. T.; S. Thomas. *Express Polym. Lett.* **2007**, *1*, 641–653.
30. Hassan, E.; Wei, Y.; Jiao, H.; Muhuo, Y. *J. Fiber Bioeng. Inform.* **2013**, *6*, 85–94.
31. Soroudi, A.; Jakubowicz, I. *Europ. Polym. J.* **2013**, *49*, 2839–2858.
32. Anastasiadis, S.H.; Gancarz, I.; Koberstein, J.T. *Macromolecules* **1998**, *21*, 2980–2987.
33. Weese, J.; Honerkamp, L. *Rheol. Acta* **1993**, *32*, 65–73.

34. Lacroix, C.; Aressy, M.; Carreau, P.J. *Rheol. Acta* **1997**, *36*, 416-428.
35. Ahmadzadeh, Y.; Babaei, A.; Gouzardi, A. *Polym. Degrad. Stab.* **2018**, *158*, 136-147.
36. López-Barrón, C.R.; Macosko, C.W. *J. Rheo.* **2012**, *56*, 1315.

GRAPHICAL ABSTRACT

